Performance Characteristics of Digitized
Spark Chambers and their Optimisation

by

A. Krolzig, R. Pforte and M. Swars

Performance characteristics of digitized

spark chambers and their optimisation

by A. Krolzig, R. Pforte and M. Swars

Deutsches Elektronen Synchrotron, Hamburg

## Abstract

At the German electron accelerator DESY, development- and pro-
duction-work has been carried out, resulting in a total of 60
wire spark chambers, mainly to equip an experiment,which is cur-
rently being run to study rho-meson production by polarized pho-
tons. Extensive use of computer installations has been made to
ensure constant production quality. Multiplane test-measurements
with on-line trackfitting enable the introduction of application
oriented parameters: Efficiency coefficients are related to the
ability of the single chamber to participate in one, two or more
tracks. The role of spurious sparks and ways to reduce them are
discussed. Accuracies of track locations and other features of
plane stacks are shown. A new arrangement for the readout of the
high voltage side is described.

The experimental arrangement for which the series of wire spark chambers has been built is shown in Fig. 1. It comprises mainly 3 telescopes surrounding the liquid hydrogen target in the forward direction of the incident gamma beam. The telescopes for the detection of the two decay-pions have 10 wireplanes each, while that for the recoil proton has 16. On the pion side directions only have to be measured, whereas in the proton arm directions and ranges must be determined.

The results of the experiment proper, rho-meson production with polarized gamma-rays, have been submitted to the high energy conference in vienna. Here, the technical aspects of producing and running such a large number of chambers, as well as the results of some more recent development shall be treated.

## Design data

The type of chamber is essentially that of J. Fisher (1). As can be seen in Fig. 1, 3 different sizes have been used. Their sensitive areas are: 256 x 416, 416 x 640 and 512 x 800 mm$^2$. The raster chosen is 1 mm. We did not consider it necessary to go to an even smaller wire distance like 0.6 mm (2) mainly for cost reasons. The gap width has been selected with 6 mm. With 20 free electrons (3), left in average by a transversing minimum ionizing particle, the efficiency is close enough to 100 % so that the higher costs for wider gaps did not seem justified. Furthermore we had to choose between stretched wire and printed wire fabrication. After trying both methods, we decided to use etched foils, since they are easier to be handled. We believe that the rejection rate would have been greater in the course of the series production using the first method. The difficulties encountered with etched foils lie in keeping the specified tolerances especially throughout the 800 mm length. Connecting as well core boards as high voltage boards by clamping them on to outlets of the chamber electrodes we had to ask for $\Delta l/l$ = 0.2/800. The mechanical accuracy of 1 part in 4000 is of course just on the limit of what can be achieved in a series production.

Finally we had to decide on the method of data retrieving.
At the time of preparing the production several authors had
shown the feasibility of using either nickel wires or coreboards
to get the coordinates of the passing particles with almost same
results. After extensive tests we found as a rule of thumb that
for large size chambers (say >1 m) and small number of sparks per
plane it is more advantageous to use nickel wire readout. For
our circumstances it was most suitable to use coreboards.
The ferrite cores have been of type Valvo 6B2. Fig. 2 shows the
behaviour of some available cores in respect of the necessary
magnetization by rectangular current pulses of various lengths
and attainable outputs at interrogation time. Note that the time-
voltage-integral is plotted instead of only voltage as is usual.
The reason is that we encountered some noise in the readout-system
so we slowed down the readout frequency to about 80 kHz (normal-
ly one finds several MHz). This is still fast enough to handle
our 3 telescopes for on-line treatment. since in signal handling
by low pass filters the v-t-integral is nearly invariant it
is here the more meaningful parameter. Another simple way to
improve the signal/noise ratio, namely using several, say 3 to 5
cores per wire, has been tried out but not used in the series
production because of difficulties of fabrication.


Measurements during production
Using a specially designed test-setup,connected to one of the
small computers (PDP5 or 8), we checked:

1. All incomming etched foils (some 140 total)
   On the average, every second one had defects, shortcircuits
   , or interrupts, which were then repaired.


2. All core-boards fabricated by a supplier. Besides short-circuits
   and interrupts wiring faults and core failures have been
   easily detected. Fig. 3 shows some statistical distribution on
   core flipping levels. Cores beyond normal limits were replaced.


3. All wire chamber after completion.
   Using cosmic rays only, we examined total efficiency, multi-
   plicity and average spark spread as a function of high voltage.
   On Fig. 4 typical values are plotted for a good chamber.

In addition, we made wiremaps, showing spark distribution per wire after some thousand events. An example is to be seen on Fig. 5. Most of the irregularities, detected in this way, could be traced back and cured. However, in 3 out of 60 cases we observed "accumulating areas" far from tolerance borders, which could not be repaired without distroying the whole chamber.

4. Finally we made gas-tests. Although after mechanical completion every chamber was checked for small holes by a helium leak detector, large differences in the efficiency could be seen after the gas flushing was turned off. The composition of the gas is the often used mixture of 70 % Ne, 29 % He, 1 % $C_2H_5OH$. Fig. 6 gives an impression of the behaviour of some chambers in this respect. To find the sources which spoil the gas we made several gas analyses with a sensitive quadrupole-type mass-spectrometer while reproducing good and bad efficiencies by more or less flushing the chambers. It seems to be established, that decreasing efficiency goes parallel with increase of the mass lines 28 and 32. In other words, undetectable leaks determine the amount of gas which must be given through in order to maintain proper operation conditions. This fact imposes severe monetary problems in cases in which a large number of chambers is to be run for months or more, because either one builds or buys an (expensive) purifying system or one buys enough bottles of fresh gas. So it seems woithwhile to improve the methods for constructing gastight chambers. Some 20 $cm^3$/min per chamber would yield a reasonable ratio of gas costs to the global cost of running an experiment. At present, our experiment needs roughly a factor of 5 to 10 more than the above figure.

Optimisation of parameters

We considerd mainly the following properties of wire spark chambers or stacks of them:
1. Efficiency, 2. Spurious sparks, 3. Spark spread,
4. Accuracy of tracks through a telescope.

## Efficiency and spurious sparks

The programs which were applied during series production, comprised among others Efficiency- and Multiplicity-counters for each chamber. The E-counter was turned up every time, one or more sparks have been found after triggering. Also, when more than one spark was found, the M-counter was turned up. This method gives a sufficiently clear picture, if a chamber out of a series is acceptable or not, even if not the best trigger conditions prevail.

During the last months, data links to the central computer (IBM 360/75) and programs became available enabling us to introduce a more precise definition of efficiency:

$$E_m = \frac{\sum_{r=1}^{n_m} k_r}{m \cdot n_m}$$

$E_m$ is the efficiency for m throughtracks, $n_m$ = number of events of type m, $k_r$ is the number of tracks, the chamber under consideration participated in at event r. Inthe FORTRAN-program acting according to this algorithm, a counter for spurious sparks will be turned up once, when one or more sparks are found which do not participate in any track.

In this way we easily found out that the amount of 10...20 % multiples, which we had normally measured along a "plateau" of roughly 1000 V, was mainly due to 5...15 % "2-prongs" or prongs of even higher order. The origin of the remaining 4...5 % stays uncertain. By scanning several hundreds of pictures, one gets the impression, that possibly the production of knock-on-electrons or maybe particles traversing only one chamber by chance coincidence could cause this effect. Fig. 7 shows a typical display with feedback from the main computer after the passage of a "5-prong" (or even a "6-prong"?).

One can assume that the 4...5 % spurious sparks could be lowered
by using less material in the particle direction if the "knock-on"
electrons dominate. We used per chamber 2 foils of epoxy rein-
forced by glassfibre, 5 mil thick, clad with 1 1/2 mil Cu.
The outer two volumes of the 3-volume-chamber are closed by 4mil
mylar foils. The biggest effect is to be expected from reducing
Cu to 3/4 mil. Other effects, leading to higher percentage of
spurious events are the well known gasimpurities and edge effects.
We made the first and the last wire 16 mm instead of 0.4 mm like
the other ones, so that they extended until the frames. To assure
low potential differences between the neighbouring wires during
pulsing, we adjusted the resistance to the first and last wire
of the high voltage side empirically to minimum efficiency.
This was in the vicinity of 0.1 % when pulsing with a fixed fre-
quency of 2 Hz.

Another attempt to increase efficiency and reduce spurious sparks
was made by applying high voltage pulses which were approximated
by pulsforming networks to an almost rectangular shape, instead
of the more usual exponential forms. This results in a slight
improvement especially in the small and medium size chambers:
In the large (512 x 800) chamber an effect is scarcely to be seen.
Probably the steep trailing edge of the rectangular pulse pre-
vents secondary sparks (growing from photoelectrons) to develop.

To study the interdependence of charge and flipped cores, we
measured the distribution over several thousand events as a func-
tion of charge and the number of flipped cores. In Fig. 8 it is
clearly to be seen that there is no abrupt end in the charge
curve towards lower values of spread. A certain number of events
falls below the trigger level for the cores, resulting in the
0.5 to 1 % misses. One easy way to reduce this number is multiple
threading of the spark wires through every core. We verified this
fact in an experimental set-up with 5-fold threading, but did
not use it in the series because of cost reasons.

## Spark spread and accuracy

Several authors (4;6) have shown, that it is possible to get
an accuracy of $\pm$ 1/4 of wire distance, in our case $\pm$ 0.25 mm.
After several thousand passages of stiff particles (in the BeV-
region), a distribution curve of delta-values proves clearly
this result. (Delta = difference of real coordinate to calculated
one by least square fit). This is true using a small area out
of the whole available one of a chamber. The curves of Fig. 9
are made with a telescope of 4 X- and 4 Y-chambers after a first
run in which lateral deviations of 0.4...0.7 mm have been detec-
ted and then corrected for by software. These small values
($\Delta = \pm$ 0.3 mm FWHM) are deteriorated by using more of the chamber
area in case of misalignments or twists along the particle axis.
Another reason is different shrinking of the foils from chamber
to chamber. Shrinking differences of 0.3 mm on the 800 mm side
are within the scope of this analysis.

A further possibility of spoiling the accuracy is the quantization
effect, first reported by Sherwood (4): If one has operation con-
ditions where doublets (spread ~ 2 mm) are prevailing, one looses
roughly a factor of 2 in accuracy. Fig. 10 shows singlets,doublets
and triplets as a fuction of high voltage. Choosing working point
WP1 (doub/sing-ratio   1) and working point WP2 (doub/sing = 8)
resp., one can verify this effect.

The curves of Fig. 10 are of course not only dependent on high vol-
tage but also very strongly on the type of high voltage coupling.
For the series of chambers we took resistive coupling with 1.8 k$\Omega$
commonly applied to groups of 8 wires of the HV-side. This arrange-
ment is relatively easy to be made and fully satisfying in cases
where only one throughtrack per telescope should be handled.
As soon as one expects more than one track especially in close
proximity, one has to choose better and more expensive means.
Fig. 11 shows a comparison of 3 arrangements: 1.8 k$\Omega$/8 mm,
1.8 k$\Omega$/1 mm and a homogeneous layer of 100 $\Omega$/square with a certain
geometrical configuration. The measurement was made in an electron
shower experiment (5). The problem can briefly be characterized

by searching for the best potential-"funnel". In Fig. 12 are plotted potential curves across the wires due to capacitive coupling along the wires during the first part of the high voltage pulse. What happens in the remaining part of the pulse duration is shown in Fig. 13: After the spark formation time of roughly 25 ns one neighbouring wire after the other breaks down, thus enlarging the current flowing to the very first point and drawing current from their own (high voltage-) wire. Fig. 14 illuminates this effect by a photograph, taken during several hundred pulses, given to the high voltage side (1.8 k$\Omega$/ 8 mm) while the group of 8 wires in the center is shortcircuited.

So, if one wants the "robbing effect" in an area as small as possible, one has to choose a coupling network which results in the optimum potential funnel. Note that in this respect stretched wires are more advantageous than etched ones as shown in Fig. 11 and 12. Also one has to emphasize, that Fig. 10 results from an experiment with isotropic distribution of sparks. One has to remember that the wires in the two planes are mounted rectangularly to each other. Multispark events occurring in one of the wire directions only will be deteriorated more or less. Thus if there is any preference in angular distribution in a multitrack experiment, a tilting of the wire planes is recommended.

## Core readout on high voltage side

Since the advantages of reading out both coordinates in one chamber are obvious (in most experiments the number of chambers and so the costs are cut down to half, as is the material in the path of the particles), we tried to get a practical and reliable solution. Normally one isolates the rather complicated wire work on the high voltage core board, since all reading and interrogating wires are at ground potential, but not the spark wires which are pulsed by up to 5 kV. The method used by us is illustrated in Fig. 15. The ferrite rings increase the inductivity in the mesh seen from the HV-pulser, so that the remaining voltage at the input to the electronics is reduced below a dangerous level. On the other hand, the interrogating and reading circuits

are not impaired because hot and ground leads run inside the ferrite rings. The skineffect in the cable sleeves improves the situation further. The insulation between wires on the high voltage board has only to withstand normal 50 to 100 V level, which is necessary for the clearing field. It is provided via the HV-pulser.

## Acknowledgements

## References

1) J. Fisher, IEEE Trans. NS-12, No.4(1965) 37.
2) Reportedly done at BNL
3) Finkelnburg, Einf.i.d. Atomphysik, 72
4) Sherwood, IEEE Trans. NS-12 (1965) 49.
5) Carried out by Mr. Vogel
6) Galster et al., Nucl.Instr. and Meth. 46 (1967)

$\pi^{(\pm)}$-Teleskope

Protonen-Teleskop

$H_2$-Target

-43°

$\pi_1^{(\pm)}$

FK

P

FK

0°

FK

FK
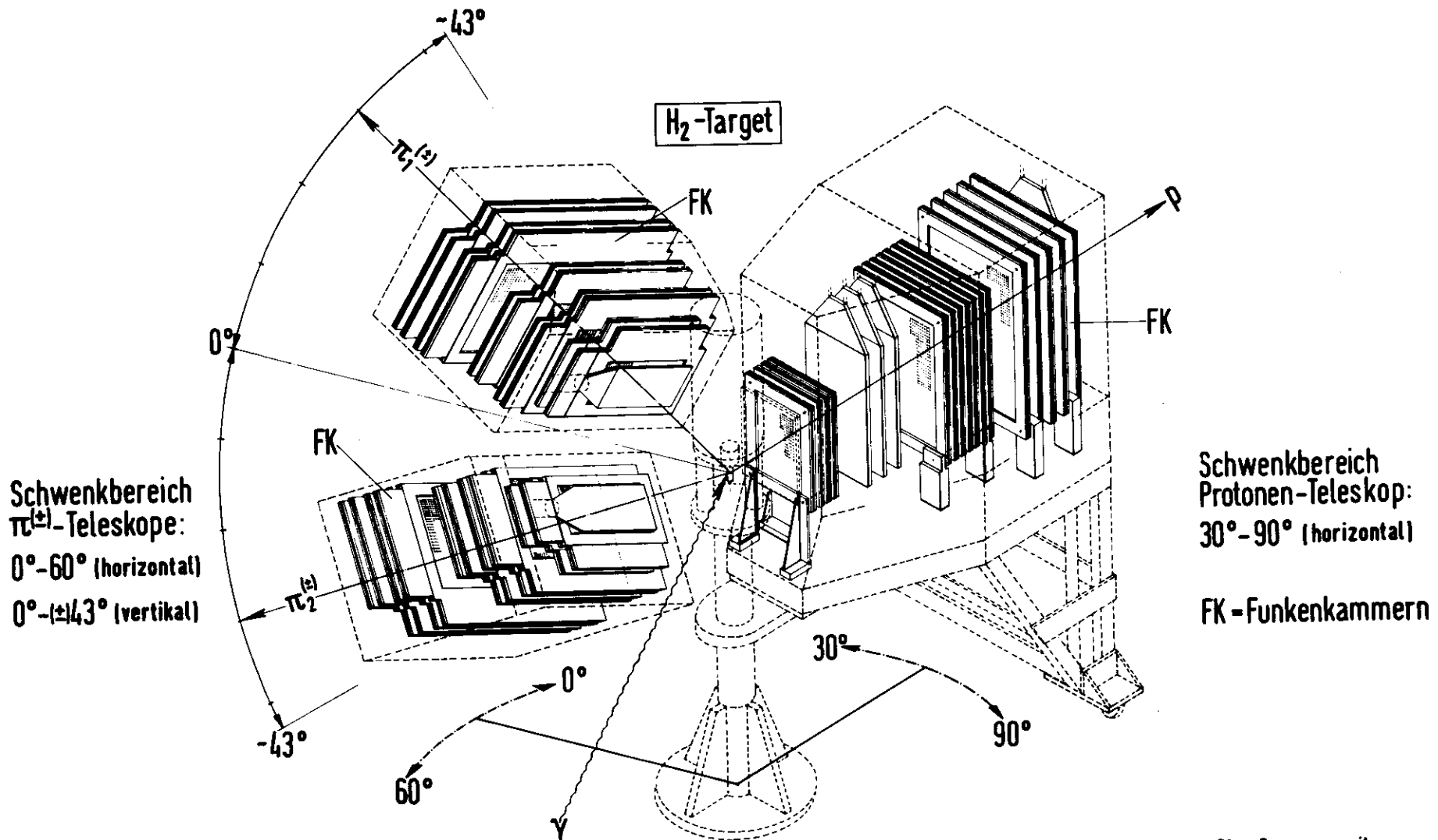
Schwenkbereich
$\pi^{(\pm)}$-Teleskope:

0°-60° (horizontal)

0°-(±)43° (vertikal)

$\pi_2^{(\pm)}$

-43°

0°

60°

γ

30°

90°

Schwenkbereich
Protonen-Teleskop:

30°-90° (horizontal)

FK = Funkenkammern

Rho-Erzeugung mit
polarisierten Photonen
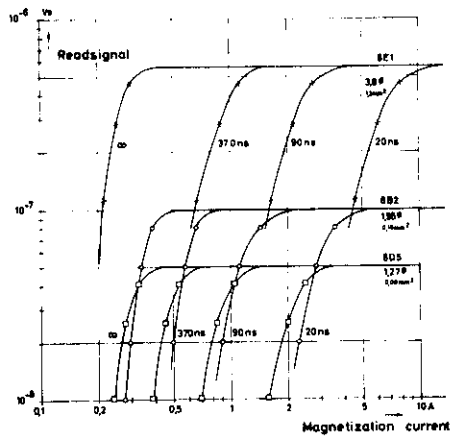
Fig. 2

Readsignal vs magne=
tizing current of 3
different memory cores
for varying pulse lengths



Fig. 3

Statistical distribution
of "flip-current" for
6B2-cores.
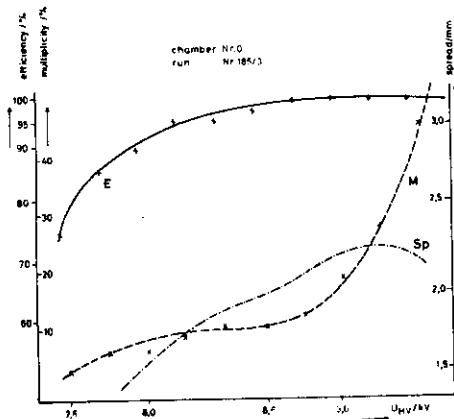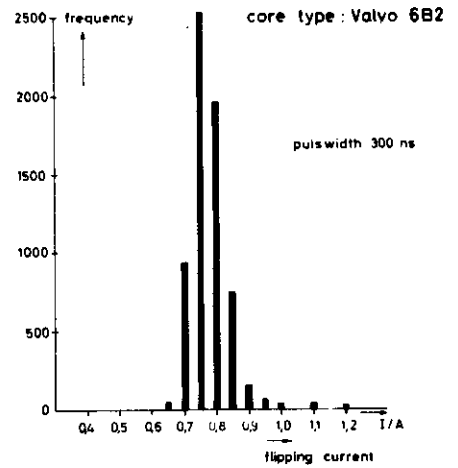
Fig. 4

Typical curves for efficiency.
multiplicity and spark spread
for a series chamber

RUN: 396   CE:   871?   E?:   8659

HAP:   5

122
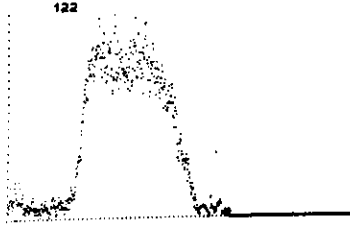
## Fig. 5

Typical wiremap for pro-
duction purposes shows
essentially the geometry
of the trigger counter.

## Fig. 6

Efficiency vs time after
gas-shut-off at different
spark chambers.

efficiency vs time after gas-shut-off

E %

Ka. Nr. 13

Ka. Nr. 11

Ka. Nr. 20

Ka. Nr. 5

Ka. Nr. 18

RUN 391   CE   498?   E?   4953

|   | X | Y |
|---|---|---|
|   | 386 | 293 |
|   | 483 | 413 |
|   | 438 | 460 |
|   | 310 | 319 |
|   | 188 | 279 |
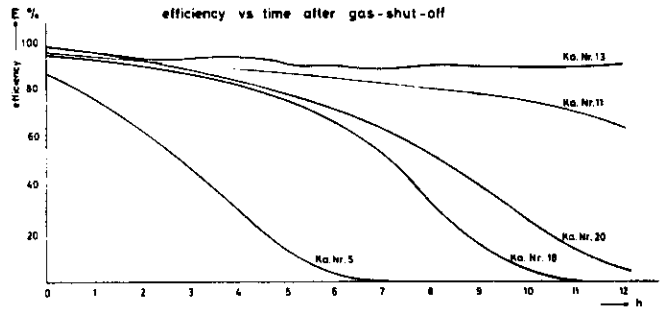
## Fig. 7

Computer representation of the
passage of a shower through a
stack of 4 X- and 4 Y-chambers
(upper and lower part of the
picture resp.).Provision is
made for 5 X- and 5 Y-chambers.

Each of the 10 chambers shown
has 6 numbers on its left with
the meaning

| | | |
|---|---|---|
| E 1 | E 2 | E 1=efficiency for |
| E 3 | E 4 | "One-track-events" |
| E 5 | Spu | Spu=spurions events |

(quoted per thousand)
The columns headed by X and Y
give the successful fittings for
1.2 ....5 prongs.
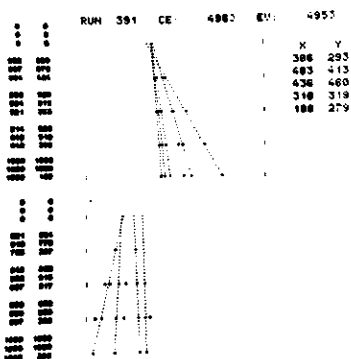
Fig. 8

Frequency as a function of charge and number of flipped cores (spread).
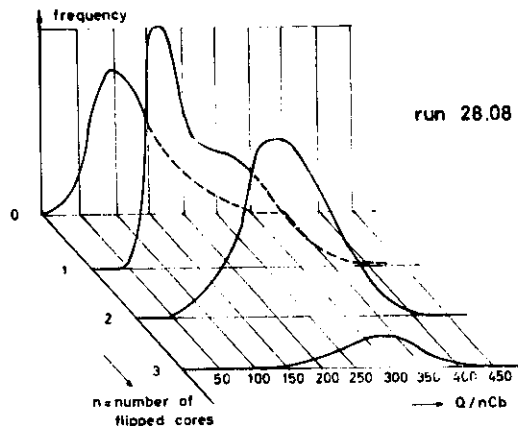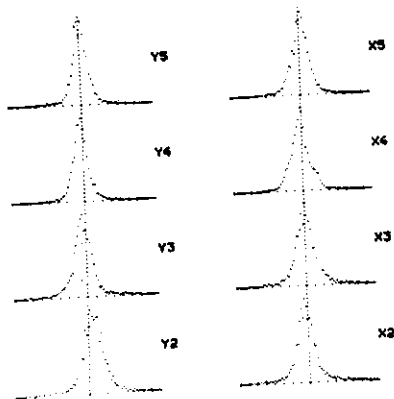


Fig. 9

Frequency of deviations from best fit for 3 X- and 3 Y-chambers. The vertical lines indicate zero deviation. The horizontal range comprises the range from -4 to +4 mm in steps of .1mm.

Fig. 10

Singlets Doublets Triplets as function of high voltage (total efficiency for orientation).

Resistances on HV-side
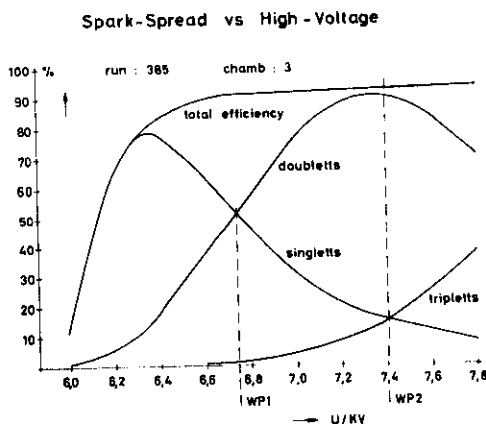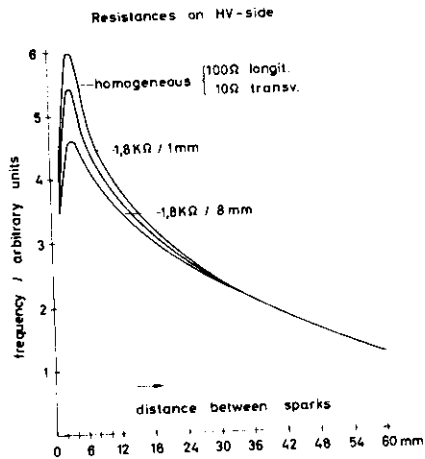


Proximity resolution of wire sparkchambers
obtained in a shower experiment.

## Fig. 11

Proximity resolution for
different resistance confi-
gurations.

## Fig. 12

Potential "funnel" at breakdown.

Potential-Funnel in 80cm-chambers at breakdown
by mutual-capacitance of wires
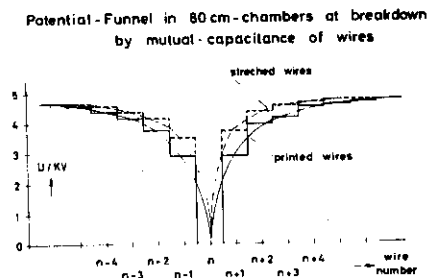


## Fig. 13

Potentials in the neighbourhood
of a spark.

Potentials in the neighbourhood of a spark
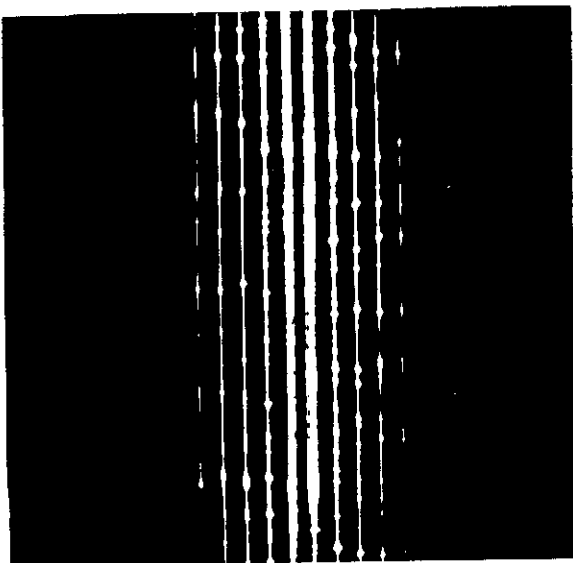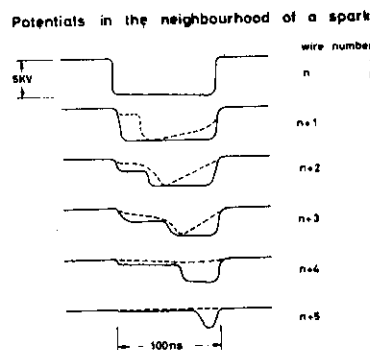




## Fig. 14

Illustration of wire-to wire
discharge.
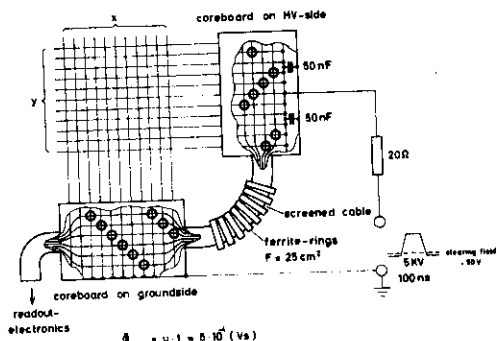
Reading x- and y-coordinates of one wire chamber
HV-isolation by means of ferrite-rings.

## Fig. 15

## HV-isolation by ferrite-rings